

Atomic structure of the *i-R*-Cd quasicrystals and consequences for magnetism

T. Yamada,<sup>1</sup> H. Takakura,<sup>2</sup> T. Kong,<sup>3,4</sup> P. Das,<sup>3,4</sup> W. T. Jayasekara,<sup>3,4</sup> A. Kreyssig,<sup>3,4</sup> G. Beutier,<sup>5,6</sup> P. C. Canfield,<sup>3,4</sup> M. de Boissieu,<sup>5,6</sup> and A. I. Goldman<sup>3,4</sup>

<sup>1</sup>*Institute of Multidisciplinary Research for Advanced Materials, Tohoku University, Sendai, Miyagi 980-9870, Japan*

<sup>2</sup>*Division of Applied Physics, Faculty of Engineering, Hokkaido University, Sapporo, Hokkaido, 060-8628, Japan*

<sup>3</sup>*Ames Laboratory, U.S. DOE, Iowa State University, Ames, Iowa 50011, USA*

<sup>4</sup>*Department of Physics and Astronomy, Iowa State University, Ames, Iowa 50011, USA*

<sup>5</sup>*University of Grenoble Alpes, SIMaP, F-38000 Grenoble, France*

<sup>6</sup>*CNRS, SIMaP, F-38000 Grenoble, France*

(Received 29 February 2016; revised manuscript received 18 July 2016; published 15 August 2016)

We report on the six-dimensional (6D) structural refinement of three members of the *i-R*-Cd quasicrystals ( $R = \text{Gd, Dy, Tm}$ ) via synchrotron x-ray diffraction from single-grain samples, and show that this series is isostructural to the *i*-YbCd<sub>5.7</sub> quasicrystal. However, our refinements suggest that the *R* occupancy on the Yb icosahedron sites within the Tsai-type atomic cluster is approximately 80%, with the balance taken up by Cd. Similarities between the *i-R*-Cd series and *i*-ScZn<sub>7.33</sub>, and their differences with *i*-YbCd<sub>5.7</sub> and *i*-Ca<sub>15</sub>Cd<sub>85</sub>, indicate that there are at least two subclasses of Tsai-type icosahedral quasicrystals. We further show from x-ray resonant magnetic scattering (XRMS) measurements on a set of closely related Tb<sub>1-x</sub>Y<sub>x</sub>Cd<sub>6</sub> 1/1 approximants that the dilution of the magnetic *R* ions on the icosahedron within the Tsai-type cluster by nonmagnetic Y disrupts the commensurate magnetic ordering in the approximant phase.

DOI: [10.1103/PhysRevB.94.060103](https://doi.org/10.1103/PhysRevB.94.060103)

Over the past 30 years, tremendous progress has been made in our understanding of the structure of quasicrystalline materials [1–4]. In particular, the discovery of a stable binary icosahedral (i) YbCd<sub>5.7</sub> quasicrystal [5] and the elucidation of the structure via six-dimensional (6D) structural refinement [6] have provided a detailed structural model of the icosahedral phase. In terms of the physical properties of quasicrystals and related compounds, recent studies have unveiled phenomena ranging from quantum critical behavior in the *i*-Yb<sub>15</sub>Au<sub>54</sub>Al<sub>34</sub> quasicrystal to bulk superconductivity in a closely related large unit cell periodic crystal (approximant), Yb<sub>14</sub>Au<sub>64</sub>Ge<sub>22</sub> [7,8]. Nevertheless, long-range magnetic order has not yet been realized in quasicrystals.

All of the known icosahedral quasicrystals with local-moment bearing elements exhibit frustration and spin-glass-like behavior at low temperatures [9,10], although numerous theoretical studies have established that long-range magnetic order on a quasilattice is quite possible [11–17]. Most magnetic quasicrystals studied to date are ternary compounds, such as *i-R*-MgZn [9,18,19], *i-R*-MgCd [9,20], and *i-R*-AgIn [21,22] ( $R = \text{rare earth metal}$ ), where chemical disorder in the local environment of the magnetic *R* ion is a complicating factor.

The recently discovered *i-R*-Cd family of magnetic quasicrystals [23], together with the cubic *RCd*<sub>6</sub> 1/1-approximants [24], comprise an ideal set of model systems for attaining a deeper understanding of magnetism in quasicrystals. Binary quasicrystals provide the compositionally simplest systems for the study of magnetic interactions in aperiodic compounds. In addition, their approximant phases manifest long-range antiferromagnetic (AFM) order at low temperature [25–29], offering the possibility for direct comparisons of the structural and magnetic properties among periodic and aperiodic phases. The *RCd*<sub>6</sub> 1/1-approximants may be described, at ambient temperature, as a body-centered cubic packing of interpenetrating rhombic triacontahedron (RTH) Tsai-type clusters, [5,24] which feature an icosahedron of

12 *R* atoms comprising the third shell of each cluster. These clusters are linked along the cubic axes by sharing a face, and interpenetrate neighboring clusters along the body diagonal.

The archetype Tsai-type *i*-YbCd<sub>5.7</sub> quasicrystal and related ternary quasicrystals [30] have been studied extensively. In particular, for *i*-YbCd<sub>5.7</sub>, the same Tsai-type clusters have been shown to comprise the backbone of the structure of the icosahedral phase with the same types of linkages, and full occupancy of the *R* icosahedron by Yb<sup>2+</sup> [6]. The Yb ions are divalent and do not carry a magnetic moment at ambient pressure [31].

For the *i-R*-Cd quasicrystals it has not yet been established whether the intercluster linkages, or even the *R* icosahedra themselves, are preserved in the icosahedral quasicrystal phase. Indeed, one interesting observation regarding these new binary quasicrystals is that their compositions vary across the heavy-*R* series from GdCd<sub>7.88</sub> to TmCd<sub>7.28</sub> [23,32], differing significantly from both the *i*-YbCd<sub>5.7</sub> quasicrystal and *RCd*<sub>6</sub> 1/1-approximants, and suggestive that these quasicrystals may comprise a new subclass of the Tsai-type icosahedral quasicrystal phases.

An important structural difference between the Tsai-type quasicrystals and their 1/1 approximants is that there is only one crystallographic site for the *R* ion in the approximant corresponding to their placement at the vertices of the icosahedron embedded in the Tsai-type cluster. For *i*-YbCd<sub>5.7</sub>, on the other hand, ~70% of the *R* ions are associated with the embedded *R* icosahedron, and the balance are contained within the double Friauf polyhedron (DFP) that fills the gap between the clusters. For the *i-R*-Cd series it was proposed that the *R* icosahedra remain intact but the DFPs are deficient in *R* [23]. It is clear, however, that a detailed description of the structure of the binary *i-R*-Cd quasicrystals is prerequisite to any comprehensive understanding of the magnetic interactions in this system, and this can only be obtained from a full structural refinement of *i-R*-Cd quasicrystals.

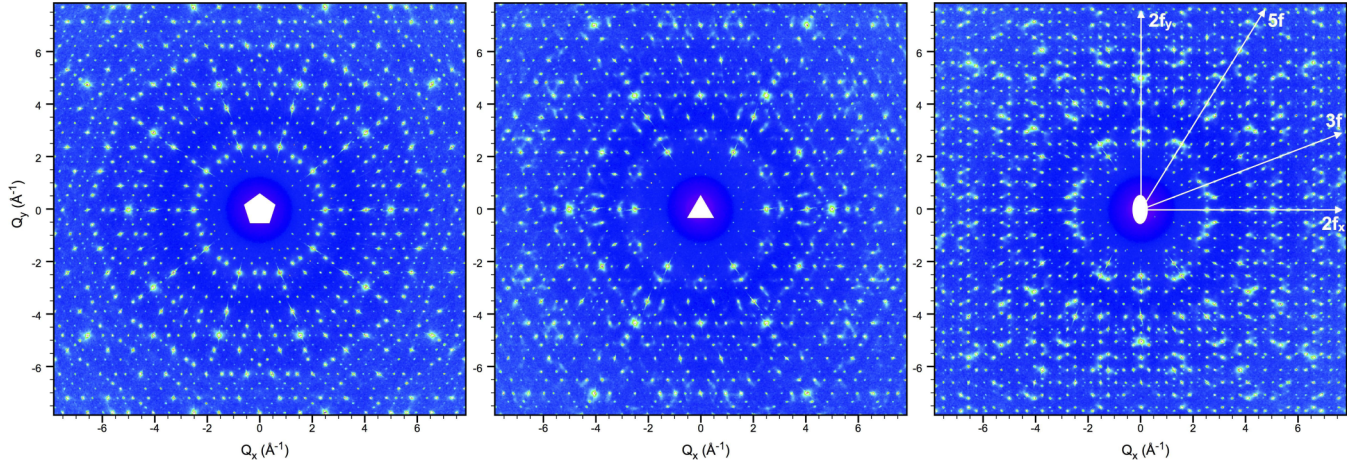


FIG. 1. Reciprocal layer reconstruction from the single-crystal x-ray diffraction for the  $i\text{-GdCd}_{7.88}$  sample showing (from left to right) the five-, three-, and two-fold planes up to  $Q = 7.85 \text{ \AA}^{-1}$ . Streaks of diffuse scattering along the three-fold direction are evident in the two-fold plane.

The  $i\text{-R-Cd}$  quasicrystals used in this study were grown from a binary melt using the solution growth method described previously [23,32,33], and subsequently annealed at  $200^\circ \text{C}$  for three days. Small single grains, approximately  $100 \times 100 \times 100 \text{ \mu m}^3$  in size, were extracted from the growths for  $R = \text{Gd}$ ,  $\text{Dy}$ , and  $\text{Tm}$  in order to sample the structural trends across the series of heavy rare earth metals. The single-crystal x-ray diffraction experiment was carried out on the CRISTAL beamline at the synchrotron SOLEIL using incident x-rays with an energy of  $24.274 \text{ keV}$  ( $\lambda = 0.51078 \text{ \AA}$ ). The details of the data collection are provided in the Supplemental Material [34]. An example of reciprocal layers reconstructed from nonattenuated single-crystal x-ray diffraction data for the  $i\text{-GdCd}_{7.88}$  sample is presented in Fig. 1.

The 6D electron densities for the  $i\text{-R-Cd}$  were reconstructed from Fourier synthesis of the structure amplitudes,  $|F| \propto \sqrt{I_{\text{obs}}}$ , with phases obtained by the low-density elimination method [35,36] using 3000 strong unique reflections common to all three samples. Figure 2 compares the electron density distribution for  $i\text{-GdCd}_{7.88}$  and  $i\text{-YbCd}_{5.7}$  [6] on a plane containing a five-fold axis in the respective 3D subspaces: the parallel (physical) space,  $E_{\text{par}}$ , and the perpendicular space,  $E_{\text{perp}}$ . Here the density was normalized by the maximum value observed near the center of the 6D primitive cubic unit cell. Even though Yb is divalent and Gd is trivalent, the overall distributions are very similar to each other indicating that the  $i\text{-GdCd}_{7.88}$  is essentially isostructural to  $i\text{-YbCd}_{5.7}$  and Gd ions are located at Yb sites (i.e., icosahedron shell and two sites on the long body diagonal of the DFP). The same features have also been found for the Dy and Tm samples. Additional plots of the 6D density distribution for all three  $i\text{-R-Cd}$  compounds are provided in the Supplemental Material [34].

Since the chemical compositions and  $R$  valency of the  $i\text{-R-Cd}$  quasicrystals are significantly different from those of  $i\text{-YbCd}_{5.7}$ , a full structure refinement [36] was carried out with all 5224 common unique reflections, based on the 6D structure model of the  $i\text{-YbCd}_{5.7}$  [6]. This was modeled by an arrangement of 3D objects called occupation domains (ODs) lying in  $E_{\text{perp}}$  and decorating the 6D periodic

lattice. The details are provided in the Supplemental Material [34].

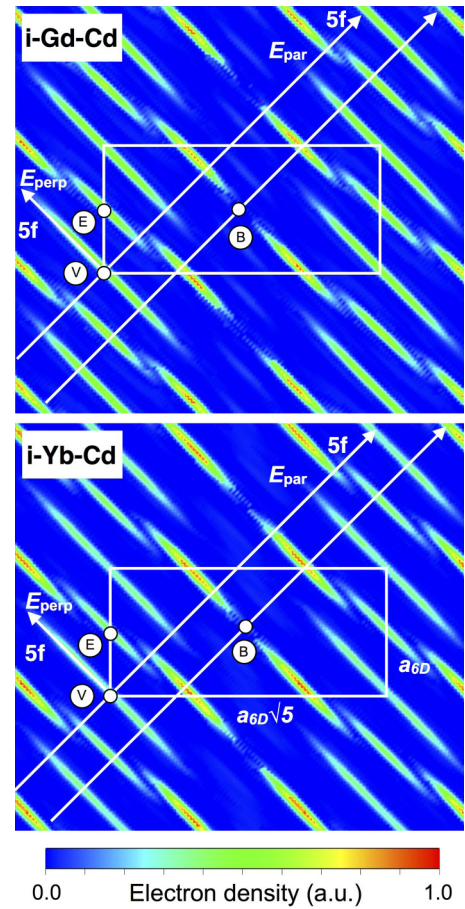


FIG. 2. Electron density distributions for  $i\text{-GdCd}_{7.88}$  and  $i\text{-YbCd}_{5.7}$  [6], on a plane containing a five-fold axis both in the parallel (physical) space,  $E_{\text{par}}$ , and perpendicular space,  $E_{\text{perp}}$ . The high symmetry positions for the 6D cubic lattice,  $(0,0,0,0,0,0)$ ,  $(1,1,1,1,1,1)/2$ , and  $(1,0,0,0,0,0)/2$ , are labeled by V, B, and E, respectively.



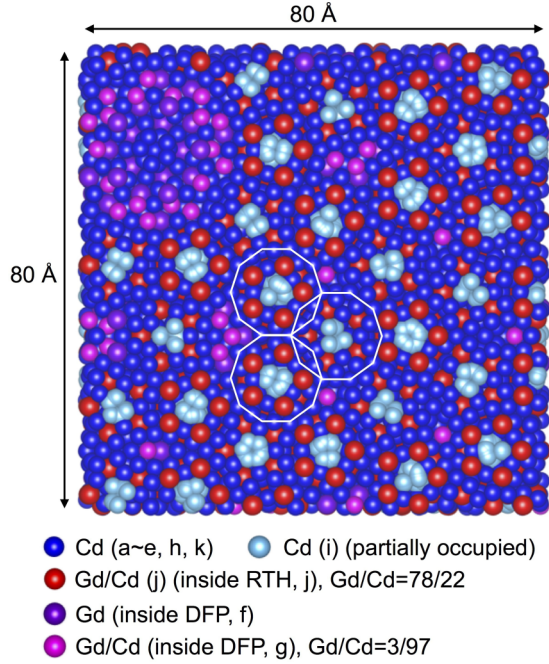


FIG. 3. A region of the refined structure of *i*-GdCd<sub>7.88</sub> in the parallel (physical) space normal to a five-fold direction. The white lines outline the positions of some of the Tsai-type clusters in the refined structure.

First, we point out that the icosahedron sites are fully occupied by Yb or *R* in the *RCd*<sub>6</sub> 1/1-approximants, the YbCd<sub>5.8</sub> 2/1-approximant and *i*-YbCd<sub>5.7</sub>. Therefore, we carried out the refinements based on a slightly modified model of the *i*-YbCd<sub>5.7</sub>, with the Yb icosahedron sites fully occupied by *R*, but allowing mixed Cd/*R* occupation of the two Yb sites in the DFP. The remaining Cd sites in the structure are preserved. The resulting reliability (*R*) factors showed reasonable values: 0.0836, 0.1028, and 0.1087 for *R* = Gd, Dy, and Tm, respectively. This further establishes that *i*-*R*-Cd and *i*-YbCd<sub>5.7</sub> have an isomorphic structure. One of the sites in the DFP (site *f* in Fig. 3 and Fig. S1 in the Supplemental Material) is mixed with Cd/*R* ratios of 100/0, 91(1)/9(1), and 76(1)/24(1) for *R* = Gd, Dy, and Tm, respectively. The other site (site *g*) is fully occupied by Cd. The refined chemical compositions for this model are GdCd<sub>7.61</sub>, DyCd<sub>7.47</sub>, and TmCd<sub>7.24</sub>, which are close to, but somewhat lower values than (especially for *R* = Gd), those determined previously using wavelength dispersive spectroscopy and magnetization measurements [23,32].

Somewhat better results for the refinements are obtained with a further modified model in which both the icosahedron and DFP sites can be occupied by Cd/*R*. The resulting *R* factors were 0.0790, 0.0997, and 0.1049 for *R* = Gd, Dy, and Tm, respectively. In this model, the icosahedron shell was found to contain *both* Cd and *R* with relative occupancies of Cd/*R* = 22(0)/78(0), 21(0)/79(0), and 18(0)/82(0) for *R* = Gd, Dy, and Tm, respectively. The refined chemical compositions are GdCd<sub>7.88</sub>, DyCd<sub>7.50</sub>, and TmCd<sub>7.28</sub>, in very good agreement with the reported values [23,32]. For the two sites in a DFP, site *f* is fully occupied by *R* and site *g* is a Cd/*R* mixed site with relative occupancies of 97(0)/3(0), 80(2)/20(2), and 81(2)/19(2) for *R* = Gd, Dy, and Tm, respectively. A slab

of the refined structure for *i*-GdCd<sub>7.88</sub>, projected onto the 3D physical space ( $E_{\text{par}}$ ), is shown in Fig. 3 illustrating the various sites and indicating some of the Tsai-type clusters. A complete list of coordinates for  $80 \times 80 \times 80 \text{ \AA}^3$  regions of the refined structures for *R* = Gd, Dy, and Tm are provided in the Supplemental Material [34]. The lower *R* factors of the refinements and closer agreement with the measured compositions suggest that the *R* icosahedra are  $\sim 80\%$  occupied by *R* in the *i*-*R*-Cd quasicrystals, with the balance occupied by Cd.

Although our analysis of the 6D electron density (Fig. 2) demonstrates the overall similarity between the atomic-scale structure of the *i*-*R*-Cd and *i*-YbCd<sub>5.7</sub> quasicrystals, there are distinct differences that are likely related to the occupancy of the *R* icosahedron. Indeed, we propose that the *R*-based binary icosahedral quasicrystals discovered so far may be grouped into two subclasses in terms of their chemical compositions and an atomic size factor given by  $\delta = r_1/r_2$ , where  $r_1$  and  $r_2$  are radii of first (larger) atom and second (smaller) atom. For reference, we note that for binary alloys the ideal  $\delta$  value for a Tsai-type cluster composed of hard-sphere atoms is 1.288 [37]. The first subclass includes *i*-YbCd<sub>5.7</sub> ( $\delta = 1.237$ ) and *i*-Ca<sub>15</sub>Cd<sub>85</sub> ( $\delta = 1.259$ ). The second subclass includes *i*-ScZn<sub>7.33</sub> ( $\delta = 1.177$ ) [38] and the *i*-*R*-Cd quasicrystals, where  $\delta$  ranges from 1.112 (for TmCd<sub>7.24</sub>) to 1.149 (for GdCd<sub>7.88</sub>). Here the  $\delta$  was calculated using the atomic radii listed in Ref. [39]. Interestingly, whereas the structural refinement of the *i*-YbCd<sub>5.7</sub> quasicrystal shows full occupancy of the *R* icosahedron shell [6], a recent 6D structural refinement for *i*-ScZn<sub>7.33</sub> also indicates the possibility of site disorder on the icosahedron shell with the ratio of Zn/Sc = 26/74 [40]. Taken together with the results presented here, this suggests a connection between smaller values of  $\delta$  and site disorder in the *R* shell of the Tsai-type cluster.

The additional phason degrees of freedom available to all aperiodic systems introduce phason fluctuations, a kind of disorder, that lead to phason diffuse scattering (PDS), which has been studied extensively in quasicrystals [41]. The *i*-*R*-Cd quasicrystals show a substantial degree of PDS in their scattering pattern, appearing as streaks oriented along the three-fold axis in *i*-GdCd<sub>7.88</sub> shown in the right-hand panel of Fig. 1. *i*-ScZn<sub>7.33</sub> presents identical diffuse streaks elongated along the same directions which are fully taken into account by PDS and a ratio of the phason elastic constants  $K_2/K_1$  equal to  $-0.53$ , i.e., close to the three-fold instability limit [40]. In a way similar to thermal fluctuations, phason fluctuations lead to a decrease of the Bragg peak intensity that is taken into account by a phason, or perpendicular, Debye Waller factor,  $B_{\text{perp}}$ . In the structure refinement, similar values of the overall  $B_{\text{perp}}$  value were obtained for *i*-*R*-Cd and *i*-ScZn<sub>7.33</sub>, that correspond to fluctuations of the OD generating the framework structure on the order 10% of their diameter.

Although the aperiodic arrangement of the Tsai-type clusters and DFPs in the quasicrystal results in a variety of local environments for the *R* ions which, in themselves, may disrupt long-range magnetic order, the observation of chemical disorder on the icosahedron sites raises the interesting question of whether this may be, in part, responsible for the spin-glass-like ground state found for the *i*-*R*-Cd binary compounds. To gain further insight into this issue we have performed low-field dc magnetization measurements on a series of the cubic

1/1-approximants,  $\text{Tb}_{1-x}\text{Y}_x\text{Cd}_6$ , and searched for magnetic ordering in these same samples using XRMS. Since there is only a single  $R$  site (the icosahedron site) in the approximant phases, these measurements allow us to probe the impact of dilution of the magnetic  $R$  ions on magnetic ordering in the approximant. The magnetization measurements were performed down to  $T = 2$  K using a Quantum Design magnetic property measurement system, superconducting quantum interference device (SQUID) magnetometer in the same manner as previous measurements on the  $i$ - $R$ -Cd series [32]. The XRMS measurements were done at station 6-ID-B at the Advanced Photon Source in the manner described previously for both  $\text{TbCd}_6$  [26] and  $\text{HoCd}_6$  [29]. The results of both measurements are displayed in Fig. 4.

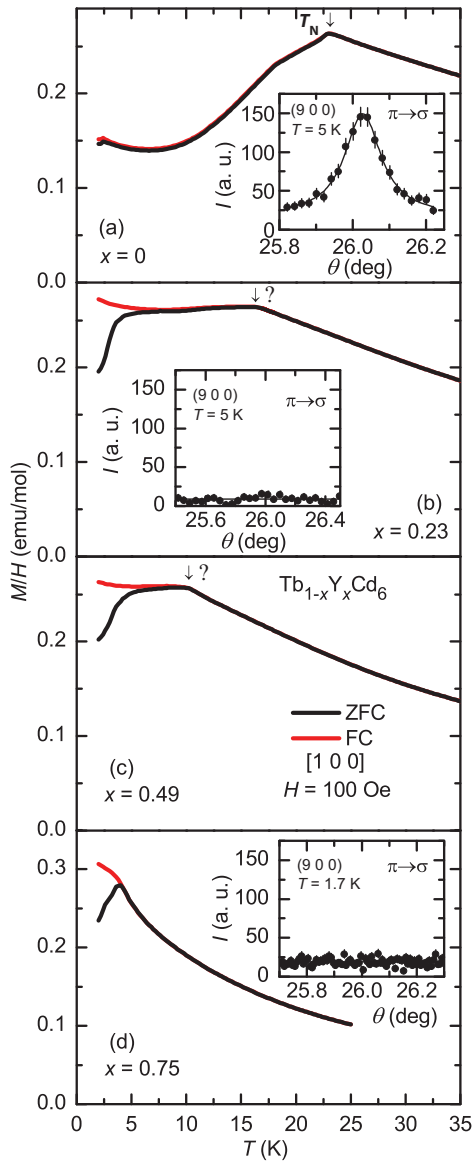


FIG. 4. Low-field magnetization data taken on the  $\text{Tb}_{1-x}\text{Y}_x\text{Cd}_6$  series as described in the text. Arrows denote the position of features in the data. Insets to panels (a), (b), and (d) show the XRMS data taken at the position of the  $(9\ 0\ 0)$  magnetic Bragg peak observed in the undiluted  $\text{TbCd}_6$  compound.

Two effects of magnetic dilution are evident in the magnetization data. First, the feature associated with the onset of magnetic order in  $\text{TbCd}_6$  appears to move to lower temperatures. The question remains, however, as to whether this feature signifies the onset of magnetic ordering in the diluted samples. Second, we find a much more pronounced separation between the field-cooled (FC) and zero-field-cooled (ZFC) data at low temperatures upon dilution of the magnetic Tb by the nonmagnetic Y. For the parent  $\text{TbCd}_6$  compound, the very slight separation at low temperatures was suggested to arise from some remaining fraction of disordered Tb moments that freeze at lower temperatures [25]. For the most dilute sample studied,  $x = 0.75$ , the plot of  $M/H$  in Fig. 4(d) is quite similar to that seen for the  $i$ - $\text{TbCd}$  quasicrystal spin-glass transition at low temperatures [32]. For  $x < 0.5$ , however, the  $M/H$  data still offer the possibility of AFM order at low temperatures.

To further study this issue we turn to the XRMS data shown as insets to the panels in Fig. 4. For the parent  $\text{TbCd}_6$  the inset to Fig. 4(a) clearly displays the long-range commensurate magnetic order described previously [26]. However, even for  $x = 0.23$  [inset to Fig. 4(b)], there is no evidence of this commensurate magnetic ordering down to the lowest temperature measured for this sample. From the present measurements we cannot exclude the presence of magnetic ordering characterized by another magnetic wave vector (e.g., an incommensurate magnetic structure). A full survey will require neutron diffraction measurements on a sample produced using a nonabsorbing Cd isotope. Nevertheless, the dilution of the magnetic Tb ions on the icosahedron sites clearly affects the magnetic interactions and changes the nature of the magnetic ordering (if present at all) even in the 1/1 approximant phase.

Finally, we recall that the dilution of  $R$  ions in the icosahedron shell within the Tsai-type clusters appears to be correlated with the ratio of the sizes of the two constituents ( $\delta \approx 1.25$  for the  $i$ - $\text{YbCd}_{5.7}$  subclass, close to the ideal value of 1.29, and a reduced value,  $\delta \approx 1.15$ , for the  $i$ - $R$ -Cd subclass). From our investigations of the closely related periodic approximant phase, we find evidence that magnetic dilution of the  $R$  icosahedron, on the order of what we have found in the  $i$ - $R$ -Cd quasicrystals, disrupts the commensurate magnetic order in the binary approximant, consistent with a degree of fragility in the magnetic ordering. This suggests that a possible path to long-range magnetic order in binary moment-bearing icosahedral quasicrystals may lie in the choice of appropriately sized constituents closer to the ideal size ratio.

We thank the synchrotron SOLEIL for the allowance of beam time for the structural measurements and P. Fertey for his help in setting up the experiment on the CRISTAL beamline. Figures 2 and 3 were obtained using VESTA software [42]. Use of the Advanced Photon Source was supported by the U.S. DOE under Contract No. DE-AC02-06CH11357. Work at the Ames Laboratory was supported by the Division of Materials Sciences and Engineering, Office of Basic Energy Sciences, U.S. Department of Energy under Contract No. DE-AC02-07CH11358. Work at Tohoku University was supported by a Grant-in-Aid for JSPS Research Fellows No. 26-2924. Work at

Hokkaido University was supported by JSPS KAKENHI No. 15K04659. Work at University Grenoble Alpes was supported

by ANR 2011-BS04-004-01. Part of this study was carried out within the European C-MAC network.

- 
- [1] T. Janssen, G. Chapuis, and M. de Boissieu, *Aperiodic Crystals. From Modulated Phases to Quasicrystals* (Oxford University, Oxford, 2007).
  - [2] W. Steurer and S. Deloudi, *Acta Crystallog. A* **64**, 1 (2007).
  - [3] M. de Boissieu, *Struct. Chem.* **23**, 965 (2012).
  - [4] A. P. Tsai, *Chem. Soc. Rev.* **42**, 5352 (2013).
  - [5] A. P. Tsai, J. Q. Guo, E. Abe, H. Takakura, and T. J. Sato, *Nature* **408**, 537 (2000).
  - [6] H. Takakura, C. Pay Gómez, A. Yamamoto, M. de Boissieu, and A. P. Tsai, *Nat. Mater.* **6**, 58 (2007).
  - [7] K. Deguchi, S. Matsukawa, N. K. Sato, T. Hattori, K. Ishida, H. Takakura, and T. Ishimasa, *Nat. Mater.* **11**, 1013 (2012).
  - [8] K. Deguchi, M. Nakayama, S. Matsukawa, K. Imura, K. Tanaka, T. Ishimasa, and N. K. Sato, *J. Phys. Soc. Jpn.* **84**, 023705 (2015).
  - [9] T. J. Sato, *Acta Crystallog.* **61**, 39 (2005).
  - [10] A. I. Goldman, *Sci. Technol. Adv. Mater.* **15**, 044801 (2014).
  - [11] C. Godrèche, J. M. Luck, and H. Orland, *J. Stat. Phys.* **45**, 777 (1986).
  - [12] R. Lifshitz, *Phys. Rev. Lett.* **80**, 2717 (1998).
  - [13] E. Y. Vedmenko, U. Grimm, and R. Wiesendanger, *Phys. Rev. Lett.* **93**, 076407 (2004).
  - [14] A. Jagannathan, *Phys. Rev. Lett.* **92**, 047202 (2004).
  - [15] S. Matsuo, S. Fujiwara, H. Nakano, and T. Ishimasa, *J. Non-Cryst. Solids* **334-335**, 421 (2004).
  - [16] S. Thiem and J. T. Chalker, *Europhys. Lett.* **110**, 17002 (2015).
  - [17] S. Thiem and J. T. Chalker, *Phys. Rev. B* **92**, 224409 (2015).
  - [18] Y. Hattori, A. Niikura, A. P. Tsai, A. Inoue, T. Masumoto, K. Fukamichi, H. Aruga-Katori, and T. Goto, *J. Phys.: Condens. Matter* **7**, 2313 (1995).
  - [19] I. R. Fisher, K. O. Cheon, A. F. Panchula, P. C. Canfield, M. Chernikov, H. R. Ott, and K. Dennis, *Phys. Rev. B* **59**, 308 (1999).
  - [20] T. J. Sato, J. Guo, and A. P. Tsai, *J. Phys.: Condens. Matter* **13**, L105 (2001).
  - [21] Z. M. Stadnik, K. Al-Qadi, and P. Wang, *J. Phys.: Condens. Matter* **19**, 326208 (2007).
  - [22] P. Wang, Z. M. Stadnik, K. Al-Qadi, and J. Przewoźnik, *J. Phys.: Condens. Matter* **21**, 436007 (2009).
  - [23] A. I. Goldman, T. Kong, A. Kreyssig, A. Jesche, M. Ramazanoglu, K. W. Dennis, S. L. Bud'ko, and P. C. Canfield, *Nat. Mater.* **12**, 714 (2013).
  - [24] C. P. Gómez and S. Lidin, *Phys. Rev. B* **68**, 024203 (2003).
  - [25] R. Tamura, Y. Muro, T. Hiroto, K. Nishimoto, and T. Takabatake, *Phys. Rev. B* **82**, 220201(R) (2010).
  - [26] M. G. Kim, G. Beutier, A. Kreyssig, T. Hiroto, T. Yamada, J. W. Kim, M. de Boissieu, R. Tamura, and A. I. Goldman, *Phys. Rev. B* **85**, 134442 (2012).
  - [27] A. Mori, H. Ota, S. Yoshiuchi, K. Iwakawa, Y. Taga, Y. Hirose, T. Takeuchi, E. Yamamoto, Y. Haga, F. Honda, R. Settai, and Y. Onuki, *J. Phys. Soc. Jpn.* **81**, 024720 (2012).
  - [28] R. Tamura, Y. Muro, T. Hiroto, H. Yaguchi, G. Beutier, and T. Takabatake, *Phys. Rev. B* **85**, 014203 (2012).
  - [29] A. Kreyssig, G. Beutier, T. Hiroto, M. G. Kim, G. S. Tucker, M. de Boissieu, R. Tamura, and A. I. Goldman, *Phil. Mag. Lett.* **93**, 512 (2013).
  - [30] T. Ishimasa, Y. Tanaka, and S. Kashimoto, *Phil. Mag.* **91**, 4218 (2011) and references therein.
  - [31] S. K. Dhar, A. Palenzona, P. Manfrinetti, and S. M. Pattelwar, *J. Phys.: Condens. Matter* **14**, 517 (2002).
  - [32] T. Kong, S. L. Bud'ko, A. Jesche, J. McArthur, A. Kreyssig, A. I. Goldman, and P. C. Canfield, *Phys. Rev. B* **90**, 014424 (2014).
  - [33] P. C. Canfield and I. R. Fisher, *J. Cryst. Growth* **225**, 155 (2001).
  - [34] See Supplemental Material at <http://link.aps.org/supplemental/10.1103/PhysRevB.94.060103> for additional experimental details, plots of the 6D density distribution and access to the CIF files.
  - [35] H. Takakura, M. Shiono, T. J. Sato, A. Yamamoto, and A. P. Tsai, *Phys. Rev. Lett.* **86**, 236 (2001).
  - [36] A. Yamamoto, *Sci. Tech. Adv. Mat.* **9**, 013001 (2008).
  - [37] T. Mitani and T. Ishimasa, *Phil. Mag.* **86**, 361 (2006).
  - [38] P. C. Canfield, M. L. Caudle, C.-S. Ho, A. Kreyssig, S. Nandi, M. G. Kim, X. Lin, A. Kracher, K. W. Dennis, R. W. McCallum, and A. I. Goldman, *Phys. Rev. B* **81**, 020201(R) (2010).
  - [39] W. B. Pearson, *The Crystal Chemistry and Physics of Metals and Alloys* (Wiley, New York, 1972).
  - [40] T. Yamada, H. Takakura, H. Euchner, C. Pay Gómez, A. Bosak, P. Fertey, and M. de Boissieu, *IUCrJ* **3**, 247 (2016).
  - [41] M. de Boissieu, *Chem. Soc. Rev.* **41**, 6778 (2012).
  - [42] K. Momma and F. Izumi, *J. Appl. Crystallogr.* **44**, 1272 (2011).